

Geochemical and Petrogenesis Studies of the granite rocks in Neoproterozoic Basement Rocks. Tagotieb area, Red Sea Hills, NE Sudan.

Satti, A, M, N^(a). K.i. Khalil^(b). Ahmed. M. El-Makky^(c).

a) Dr. Albarra .M.N. Satti. Mining and Economic Geology Department , Faculty of Earth Sciences, Red Sea University. Sudan. albarrasatti78@yahoo.com

(b)Prof. Dr. Khalil I. Khalil Geology Department, Faculty of Science Alexandria University. Egypt. kebeid@yahoo.com

(c)Prof .Dr. Ahmed M. ElMakky, Department of Geological and Biological Sciences, Faculty of Education, Alexandria University. Egypt. ahmedelmakky@yahoo.com

Abstract

Active crustal accretion in the form of syn- to post orogenic igneous activity characterized the late Proterozoic of NE Sudan, and gave rise to the thermal overprinting of many pre-existing rocks (Klemencic & Poole 1985, Vail 1988). Petrographically syn-tectonic granitoids are composed of quartz, plagioclase feldspar, alkali feldspar, biotite, hornblende, and accessory zircon, sphene, iron oxides and apatite.. The post-orogenic granites are of pink colour, coarse-grained, non-foliated, and contain quartz, plagioclase and K-feldspar with little amount of mica and hornblende. The syn-orogenic granitoids show chemical characteristics of calc-alkaline subduction-related rocks and can be regarded as I-type granites. The geochemical data show marked continuities in major and trace element abundances versus SiO₂ suggesting that all varieties of the syn-tectonic granodiorite-granite suite are genetically related. The primitive nature of the original magma that produced the studied granodiorite-granite suite is evident from the very low Rb/Sr (0.09–0.35), Nb (3–7 ppm), which reflect either garnet lherzolite mantle source or amphibolites lower crust source. On the basis of geochemical variations, it is suggested that crystal fractionation and fluid–rock interaction are the main control of the trace element distribution in the studied post-orogenic A-type granites. The petrogenesis studies show that the ferroan character and the overall alkalic to alkali-calcic affinities of most rocks are consistent with the original definition of A-type granitoids proposed by Loiselle and Wones (1979) and as emphasized by Frost and Frost (2001). It is suggested that the studied A-type granites were generated by partial melting of a young crustal source, with subsequent fractionation of feldspars and mafic minerals during magmatic evolution. These melts are related to decompression melting due to erosional uplifting following lithospheric delamination during the post-collisional stage of the ANS evolution. For the studied granites, plotting ratios of K/Rb, Zr/Hf, and Sr/Eu versus the TE_{1,3} (tetrad effect) and strong decrease in Eu concentrations with tetrad effect ,suggested that crystal fractionation and fluid–rock interaction are the main control of the trace element distribution in the studied post-orogenic A-type granites.

Keywords: Tagotieb , granite, syn tectonic, post granite and A-type granites

1-Introduction:

The Tagotieb area is located in the southern part of the Red Sea Hills, northern Sudan. It occurs at about 80 km to the northwest of the Sudanese Eritrean boundaries. Syn – to late orogenic intrusives widely known as “batholithic granites” or granitoid plutons are composed dominantly of foliated tonalities, granodiorite and granites which occupy more than 60% of the exposed area in the northern Red Sea Hills. These intrusions represent the oldest intrusive in the area (Nour, 1983). The granitoid

masses are characterized by coarse grained textures. These granitic rocks are highly sheared and affected by numerous faults and joint. All the contacts between granitoid plutons and volcano sedimentary – sequences (host rocks) in most cases occur along zones of weakness showing regional trends along which Khors and Wadies are now developed (Nour, 1983). Syn–orogenic intrusions are composed dominantly of foliated tonalite, granodiorite and granite, but the post-orogenic complexes are mainly composed of pink alkaline granite, gabbro, and dykes. The post-orogenic intrusions have been divided into three phases; the first and second are associated with the Pan African geotectonic thermal events, but the third phase is clearly undeformed and more alkaline in composition (Nour, 1983). In this paper, we report geological and geochemical data of Neoproterozoic granitoid intrusion (Derudieb area, Red Sea Hills. Sudan), which tectonically locates in the Haya terrain. The main aim is to study the geochemical features and evolution their tectonic setting, also to identify the genesis of the granite rocks in the study area

1.2 Research Methodology:

Research methodologies, which are used to accomplish the objectives of the present work, are mainly: (1) fieldwork and sampling of the different rock units (2) preparation of thin sections for most of the collected samples (13) and chemical analyses of major, minor and trace elements. In the field, sampling was conducted by collecting representative rock specimens from specific outcrops in the study area. These specific outcrops include syn tectonic granite (8 samples) and post tectonic granite (5 samples) (Table 1.1).

13 samples were analyzed for major and some selected trace elements by inductively coupled plasma mass spectrometry (ICP-MS). The remaining trace elements and rare earth elements (REE) were analyzed by inductively coupled plasma-atomic emission spectrometry (ICP-AES). All the analyses were carried out at the ACME Analytical Laboratories Ltd., Canada. From petrogenetic studies, we select 13 samples to be analyzed (package LF200- AQ200) in the Acme Lab, to determined major, trace and RRE elements. After fusion of 0.2g of the powdered sample by LiBO₂, major element compositions and Sc, Ba, and Ni abundances were determined by inductively coupled plasma-atomic emission spectrometry (ICP-AES). The remainder of trace elements and the rare earth elements (REE) were determined by inductively coupled plasma-mass spectrometry (ICP-MS).

Table 1. The coordinates of the samples collected from the study area.

Sample Number	Latitude	Longitude
B 11	36.34783333	17.62711111
B 6-2	36.34194444	17.63447222
C 19	36.2575	17.53244444
B 7-1	36.35938889	17.61552778
D 5	36.14980556	17.53652778
D 1	36.16666667	17.51055556
B 9	36.365	17.61841667
B 13	36.29166667	17.55861111
A1	36.23861111	17.55055556
B 3	36.28666667	17.63638889
C 18	36.25936111	17.52888889
B 6-1	36.34194444	17.63447222
A3	36.23861111	17.55055556

1.2 Geological setting:-

Active crustal accretion in the form of syn- to post orogenic igneous activity characterized the late Proterozoic of NE Sudan, and gave rise to the thermal overprinting of many pre-existing rocks (Klemenic & Poole 1985, Vail 1988).

The area is predominantly comprised of late a Proterozoic metavolcano-sedimentary sequence, which was previously known as the Nafirdieb Formation. The metavolcano-sedimentary rocks are intruded by gabbros and several granitoid phases including syn- and post-orogenic granitoids Fig (1.1).

1.2.1 Syn-tectonic Granite:

The study area has been extensively intruded by syn- to late-tectonic plutons, which are intruded into the metavolcano-sedimentary sequence and vary in rock composition from granodioritic to granitic. Granodiorite occurs in the southwest and northern part of the study area. In the southwestern part, the granodiorite occurs as elevated outcrops intruding low grade metamorphosed metavolcano-sedimentary rocks. Near Khor Derudieb, in the central part of the area, granodiorite occurs as moderately elevated outcrops. The rocks are typically greenish grey in colour with feldspar phenocrysts and relatively high mafic contents. Syn-tectonic granite intrusions cover several parts with low relief and highly dispersed boulders.

In the central part of the study area, foliated granites occur as large boulders with well-developed exfoliation phenomena. These granite boulders are highly weathered, rounded, and lies with its long axis parallel to the regional foliation. In the bank of Khor Dageint , there are outcrops of syn-tectonic granite rocks that occur as highly elevated hills and boulders with an exfoliation surface. These rocks are typically grey to black in color and rich in mica minerals.

1.2.2 Post-tectonic granite

The post-tectonic intrusions were intruded during the late Pan-African events. They are considered as the youngest Precambrian magmatic rocks that are usually non-foliated and unmetamorphosed (Abu Fatima 1992). The Post-tectonic granites in the study area occur as irregular outcrops, which are tabular to circular in form. They are randomly dispersed throughout the study area and were intruded into all older rock units. Near Jeble Wangarmy, in the northwestern part of the study area, there is a moderately elevated granite intrusion that occurs in a dome-like form and is rich in potash feldspar with some veinlets of silica. Furthermore, these rocks are mostly dissected by irregular two sets of joints. In the bank of Khor Awagtieb there is a high elevated outcrop of post-tectonic granite in the form of massive mass with some joints. Most of the post-tectonic granite outcrops in the study area are cut by several basic dykes such as andesite or dolerite.

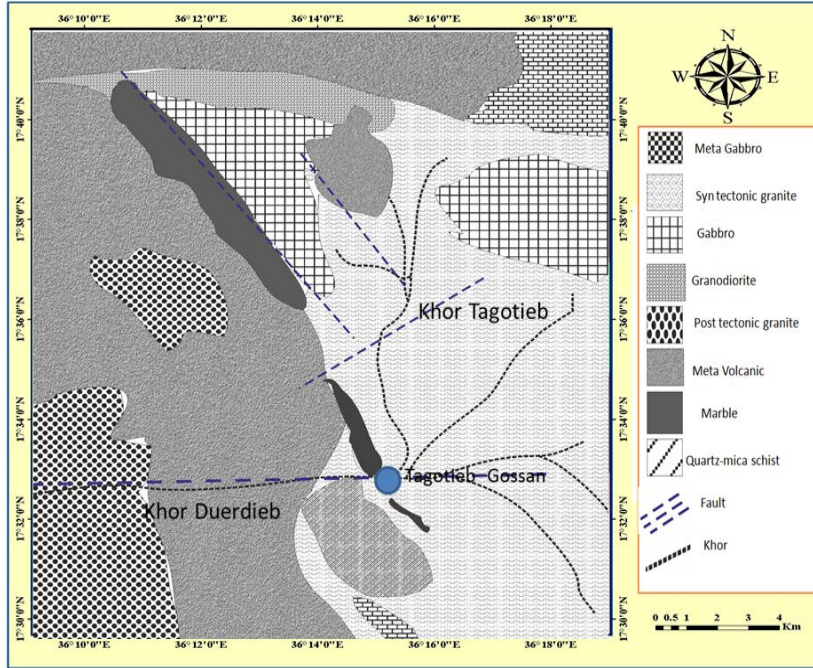


Fig. 1.1. Simplified geological map of the study area.

2.1. Geochemistry of the Granite Rocks

The geochemical data of major, trace and rare earth elements of 13 representative samples of the studied granite rocks are given in Table 1.1. The syn-orogenic granitoids and post-orogenic granite are discussed here together to depict differences in their chemical characteristics and tectonic setting. Using the Q-ANOR diagram of (Streckeisen and Le Maitre 1979), the data points of the syn-orogenic granitoid plot in the granodiorite and monzogranite fields, whereas samples of the post-orogenic granite indicate a syenogranite to alkali feldspar granite composition (Fig. 2.1).

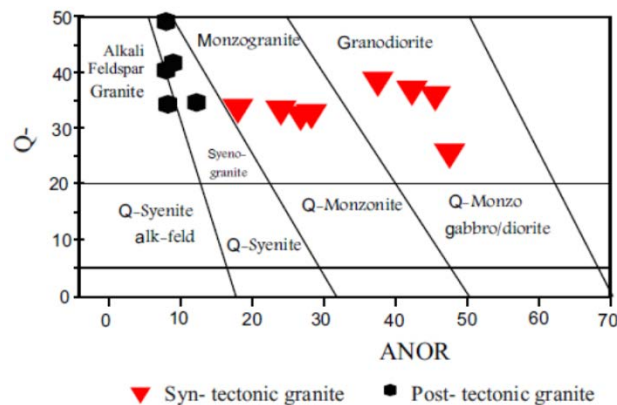


Fig. 2.1: Q - ANOR geochemical classification diagram for the studied granitoid rocks Streckeisen and Le Maitre (1979). Q and ANOR are calculated using norm values: $Q = 100 / (Q + Qr + Ab + An)$, $ANOR = 100An / (An + Qr)$.

Characteristically, the syn-orogenic granitoids have higher Al_2O_3 , MgO , CaO , Fe_2O_3 , TiO_2 , Ba , Zr , and V , but lower total alkalis, SiO_2 , Th , U , and REE , compared to the post-orogenic granite (Table 2). The Harker variation diagrams of some major elements abundances show trends of increasing K_2O and Na_2O and decreasing MgO , CaO , Fe_2O_3 , and TiO_2 with increasing SiO_2 (Fig. 2.2 & 2.3).

	Syn tectonic granite							
	B11	B6-2	C19	B7-1	D5	D1	B9	B13
SiO ₂	66.52	73.06	71.35	73.46	73.80	73.14	71.95	71.73
TiO ₂	0.70	0.37	0.35	0.24	0.28	0.32	0.32	0.41
Al ₂ O ₃	15.37	13.44	13.53	13.75	13.48	13.86	14.03	13.94
Fe ₂ O ₃	4.47	2.77	2.55	1.63	2.20	2.19	2.50	2.62
MnO	0.08	0.05	0.09	0.03	0.07	0.07	0.11	0.05
MgO	1.39	0.72	0.65	0.36	0.47	0.53	0.86	0.66
CaO	3.27	1.98	1.75	1.28	2.15	2.27	1.36	1.91
Na ₂ O	4.29	3.83	3.80	3.45	4.25	4.38	4.40	3.74
K ₂ O	2.74	2.70	3.89	4.86	2.41	2.23	3.18	3.87
P ₂ O ₅	0.22	0.11	0.11	0.06	0.07	0.07	0.16	0.14
LOI	0.6	0.7	1.6	0.7	0.7	0.8	0.9	0.6
Sum	99.65	99.73	99.67	99.82	99.88	99.86	99.77	99.67
Cr	116	130	328	95	109	68	136	116
Ni	7.7	5.9	8.1	3.5	2.7	2.6	5.6	3.5
Sc	8	5	5	3	5	6	7	5
Ba	1530	1467	1424	897	456	456	868	1663
Be	7	3	5	4	4	2	4	<1
Co	9.1	4.9	4.9	2.6	3.9	3.4	4.1	4.6
Cs	0.2	0.5	0.2	0.2	0.5	0.7	0.6	0.2
Ga	20.1	17.5	18.0	16.5	14.6	14.8	19.0	18.1
Hf	7.8	6.6	5.1	4.7	4.4	4.0	5.3	7.1
Nb	7.8	2.9	6.0	3.8	6.7	7.0	6.0	6.9
Rb	43	37	57	66	59	49	59	57
Sn	3	1	2	1	2	2	2	2
Sr	484	286	239	199	203	210	167	313
Ta	0.6	0.1	0.6	0.2	0.6	0.6	0.4	0.6
Th	3.9	2.9	4.5	4.8	3.2	2.6	6.7	5.1
U	1.5	0.7	1.2	0.8	1.1	0.9	1.0	1.0
V	68	43	36	23	30	27	29	39
W	0.5	1.2	<0.5	<0.5	1.3	0.9	1.1	0.8
Zr	328	247	181	164	168	148	187	261
Y	29	9	25	5	26	29	44	21

	Post tectonic granite				
	A1	B3	C18	B6-1	A3
SiO ₂	78.91	75.68	77.53	76.12	76.00
TiO ₂	0.20	0.03	0.07	0.03	0.27
Al ₂ O ₃	9.86	13.96	12.26	13.29	11.35
Fe ₂ O ₃	2.93	0.53	0.88	0.64	3.16
MnO	0.03	0.06	0.04	0.21	0.02
MgO	0.03	0.05	0.08	0.05	0.03
CaO	0.46	0.48	0.46	0.65	0.45
Na ₂ O	2.54	4.49	3.79	4.41	3.43
K ₂ O	4.30	4.04	4.42	4.02	4.39
P ₂ O ₅	0.02	0.04	0.02	<0.01	0.01
LOI	0.6	0.6	0.4	0.5	0.8
Sum	99.88	99.96	99.95	99.92	99.91
Cr	68.43	82.11	88.94	130.08	75.27
Ni	2.9	2.8	2.2	2.2	1.7
Sc	<1	4	4	10	1
Ba	128	24	54	39	137
Be	<1	2	7	10	1
Co	2.2	1.9	1.6	1.5	1.4
Cs	<0.1	0.9	0.1	0.6	0.2
Ga	19.9	26.5	20.1	22.9	21.8
Hf	8.3	3.7	4.2	5.6	8.1
Nb	10.6	28.4	8.3	25.4	11.1
Rb	25.7	193.1	82.0	134.0	27.1
Sn	1	4	1	2	1
Sr	11.6	10.1	12.3	11.9	9.7
Ta	0.4	4.5	0.4	2.9	0.4
Th	2.4	10.7	8.8	11.0	0.7
U	0.7	10.1	2.0	18.2	0.5
V	32	13	18	21	14
W	<0.5	1.0	0.8	1.0	<0.5
Zr	534.7	28.0	76.9	82.0	493.2
Y	27.8	38.4	48.6	118.5	21.2

Table 2. Geochemical data of major (wt %) and trace elements (ppm) for the studied granites.

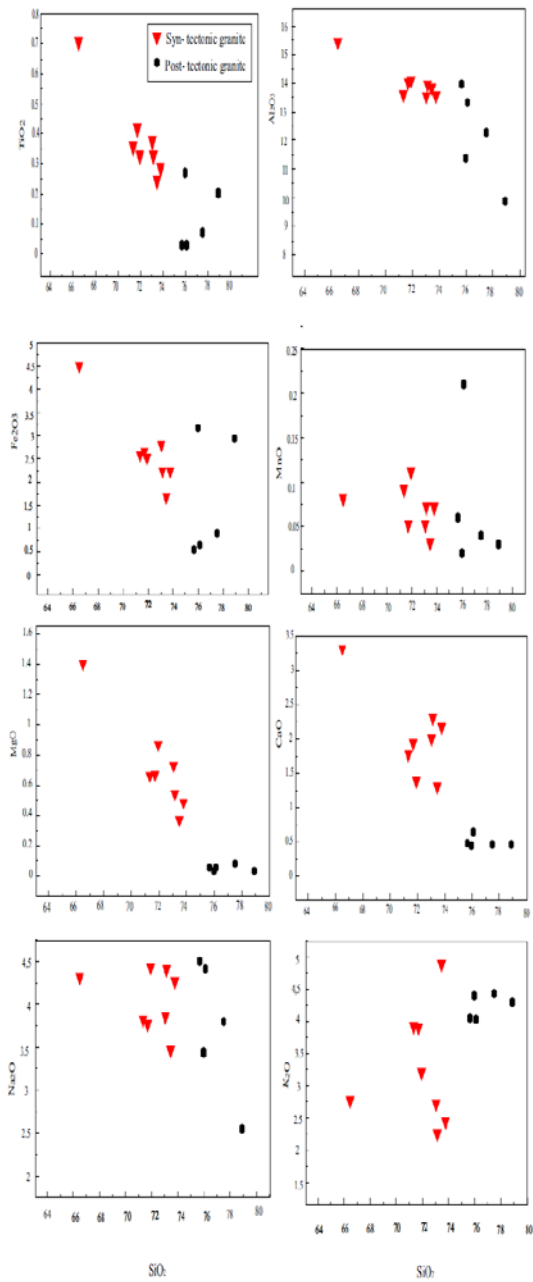


Fig. 2.2: Harker variation diagram for major element oxides of granitoid rocks in the study area.

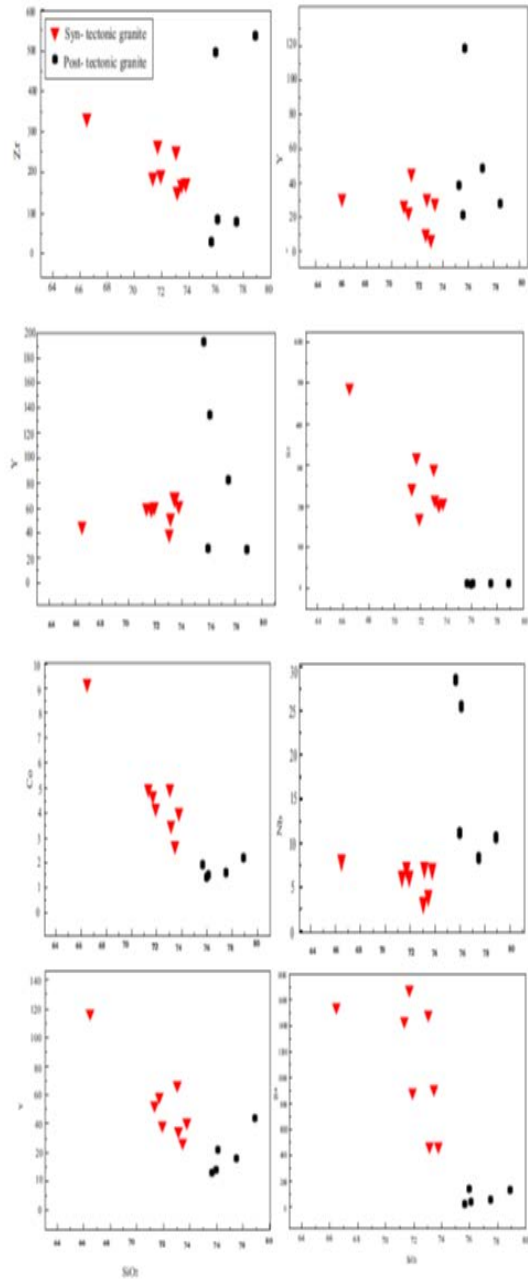


Fig. 2.3: Harker variation diagram for some trace elements vs. SiO₂ of granitoid rocks in the study area.

2.2. Fractional crystallization:

The trace element contents show slightly clear trends in the investigated syn- to post-tectonic granite rocks. The large ion lithophile elements (LILE) Ba and Sr show geochemical behavior indicating fractionation of a mineral assemblage rich in plagioclase and K – feldspar, which would cause depletion of melt in Ba and (Moghazi 1994). The variation diagrams shows increasing of Ba with increasing SiO₂ in post-tectonic granite due to plagioclase fractionation (Hall 1987).

Table 3. REE elements data of the granitoid rocks in the study area.

	Syn tectonic granite								Post tectonic granite				
	B11	B6-2	C19	B7-1	D5	D1	B9	B13	A1	A3	B6-1	C18	B3
La	37.2	30.2	35.5	34.9	13.6	19	24.5	44	52.3	26.6	2.9	11.1	5.9
Ce	78.9	49.3	67.8	62.1	27.2	41.1	50.5	91.8	118.9	56.4	7.2	36.3	15.9
Pr	9.32	5.66	7.7	6.29	3.33	5.23	6.79	10.45	14.24	7.3	0.86	4.85	1.96
Nd	34.7	19.4	27.8	19.6	13.1	19.9	27.8	36.4	57.2	29.2	3.9	20.6	7.8
Sm	7.06	3.17	5.81	2.68	3.24	4.44	6.93	5.93	10.08	5.13	2.5	7.04	4
Eu	1.8	1.26	0.97	0.81	0.99	1.08	1.6	1.42	0.92	0.9	0.19	0.27	0.21
Gd	6.26	2.71	5.06	2.19	3.92	4.8	7.41	5.28	7.78	4.68	5.95	7.87	4.74
Tb	0.93	0.35	0.81	0.22	0.66	0.79	1.29	0.74	1.1	0.73	1.75	1.53	1.05
Dy	5.61	1.79	4.56	1.15	4.11	4.75	7.61	3.76	5.66	4.01	14.33	9.15	6.29
Ho	1.04	0.32	0.93	0.2	0.97	1.03	1.53	0.77	1.05	0.84	3.65	1.98	1.33
Er	2.94	0.99	2.44	0.59	2.97	3.23	4.71	2.33	3.07	2.52	12.3	5.7	3.89
Tm	0.45	0.15	0.38	0.09	0.47	0.52	0.71	0.34	0.5	0.33	2.23	0.86	0.66
Yb	3.03	0.96	2.62	0.67	3.39	3.86	4.78	2.39	3.57	2.39	17.21	5.16	4.96
Lu	0.45	0.16	0.37	0.12	0.54	0.57	0.75	0.39	0.61	0.36	2.83	0.72	0.73
ΣREE	189.69	116.42	162.75	131.61	78.49	110.3	146.91	206	276.98	141.39	77.8	113.13	59.42
(La/Yb)_n	8.81	22.57	9.72	37.36	2.88	3.53	3.68	13.21	10.51	7.98	0.12	1.54	0.85
(La/Sm)_n	3.40	6.15	3.94	8.41	2.71	2.76	2.28	4.79	3.35	3.35	0.75	1.02	0.95
(Gd/Yb)_n	1.71	2.34	1.60	2.70	0.96	1.03	1.28	1.83	1.80	1.62	0.29	1.26	0.79
(Eu/Eu*)	0.83	1.31	0.55	1.02	0.85	0.72	0.68	0.78	0.32	0.56	0.15	0.11	0.15

The abundance of the rare earth elements (REEs) in the different granite types of the study area is given in Table 1.2 and their variation and behavior are manifested as Chondrite-normalized REE patterns (Fig.2.4 a,b) with chondritic values from Sun and McDonough (1989). In general, there is a pronounced increase in the ΣREE, decrease of LREE fractionation and depth of the Eu anomalies from the syn-orogenic to the post-orogenic granites. The syn-orogenic granite samples are characterized by high fractionated REE patterns (La/Yb_n = 3.53 – 37.4), lowest total REE content (Σ REE = 78 – 206ppm), and flat to moderately fractionated HREE (Gd/Yb_n = 1.0 - 2.7). This indicates that HREE-bearing minerals such as garnet and/or zircon are not

fractionated phases during the crystallization of granodiorite. Except two samples, which have positive Eu-anomalies ($Eu/Eu^* = 1.02$ and 1.31), most samples of the syn-tectonic granites exhibit small negative Eu – anomalies ($Eu/Eu^* = 0.85 - 0.55$).

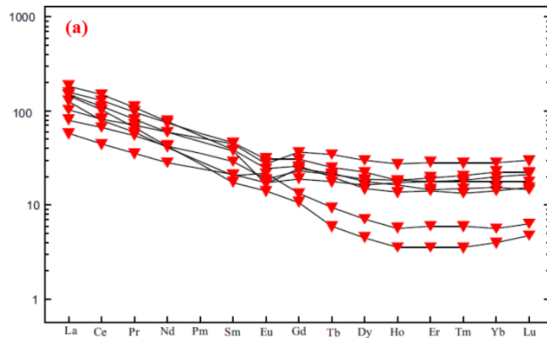


Fig. 2.4 a: Chondrite-normalized REE patterns of the syn-tectonic granitoids in the study area.

Normalizing values are from Sun and McDonough (1989).

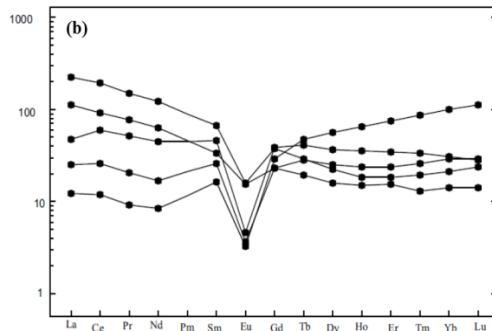


Fig. 2.4 b: Chondrite-normalized REE patterns of the post-tectonic granitoid rocks in the study area.

Normalizing values are from Sun and McDonough (1989).

Despite some discrepancies in the elements enrichment/depletions, the rocks of the syn-tectonic granites are collectively enriched in the LIL elements and have high LILE/HFSE ratios and significant Nb, Sr, Ti and Th negative anomalies. These chemical features are common and characterize arc-related magma (Pearce et al., 1982,) or granites derived from a crustal source, which itself were derived from arc crust (Whalen et al., 1987). Such anomalies also emphasize the role of feldspar and Fe-Ti oxides separation during the crystallization of these rocks. Compared with the syn-tectonic granites, the post-tectonic granites show high contents of trace elements and close similar patterns with strong development of negative K, Ba, Sr, and Ti anomalies. This marked depletion would be consistent with a greater degree of fractionation of K- feldspar, apatite and Fe- Ti oxides (Moghazi 1994).

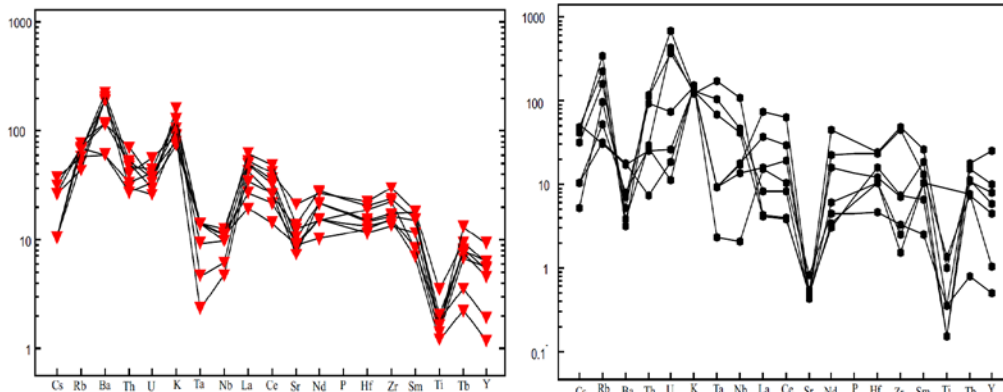


Fig. 2.5: Mantle-normalized trace- element spider-diagrams (Wood, 1979) for the studied granitoid samples.

2.3. Magmatic evaluation:

The magma type and tectonic setting of the studied granitoid rocks will be discussed using some discrimination diagrams such as $100(MgO + FeO + TiO_2 + SiO_2)$ vs. $(Al_2O_3 + CaO/FeO + Na_2O + K_2O)$ discrimination diagram (Sylvester, 1998) and Nb vs. Y , Rb vs. Y+Nb, Rb vs. Y+Ta and Yb vs. Ta diagrams of(Pearce et al 1984).

On the $100(\text{MgO} + \text{FeO} + \text{TiO}_2 + \text{SiO}_2)$ vs. $(\text{Al}_2\text{O}_3 + \text{CaO}/\text{FeO} + \text{Na}_2\text{O} + \text{K}_2\text{O})$ diagram (Fig. 2.6) of (Sylvester 1998), the syn-tectonic granite samples lie in the field of calc-alkaline granite, but most of the post-tectonic granite samples plot in the field of alkaline and highly fractionated calc-alkaline granites. According to the $\text{K}_2\text{O} - \text{Na}_2\text{O} - \text{CaO}$ ternary diagram (Barker and Arth, 1976), all the granitoid samples follow the calc-alkaline trend, but the alkali feldspar granite samples lie near the $\text{K}_2\text{O} - \text{Na}_2\text{O}$ line, which may indicate more alkaline character (Fig. 2.7).

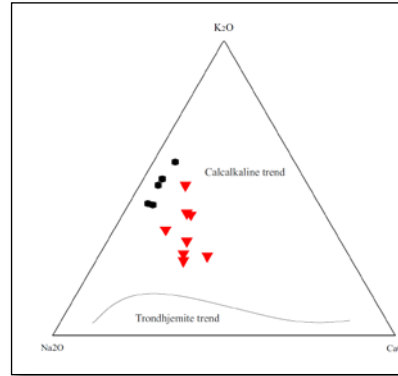
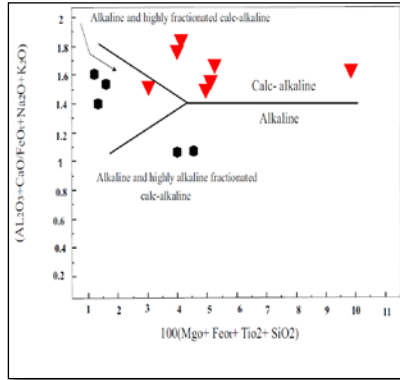


Fig. 2.6. $100(\text{MgO} + \text{FeO} + \text{TiO}_2 + \text{SiO}_2)$ vs. $(\text{Al}_2\text{O}_3 + \text{CaO}/\text{FeO} + \text{Na}_2\text{O} + \text{K}_2\text{O})$ discrimination diagram (Sylvester, 1998) for the studied granitoid rocks.

Fig. 32.7: $\text{K}_2\text{O} - \text{Na}_2\text{O} - \text{CaO}$ ternary diagram (Barker and Arth, 1976) showing all the studied granitoid samples follow the calcaline trend.

On the Rb vs. $\text{Y} + \text{Nb}$, Rb vs. $\text{Y} + \text{Ta}$ and Yb vs. Ta (Fig. 2.8) of (Pearce et al 1984), the syn tectonic granite samples fall in the volcanic arc granite (VAG) field. The post-tectonic granites plot in both the volcanic arc granite (VAG) field and the within-plate granite (WPG) field but most samples lie within (VAG).

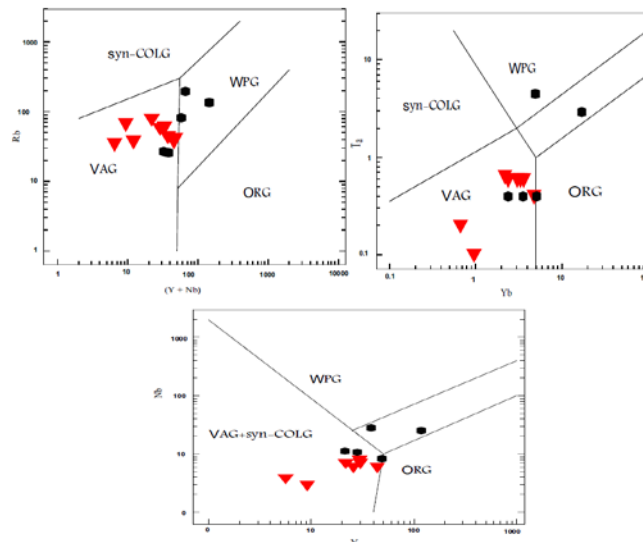


Fig. 2.8: Tectonic discrimination diagrams for the studied granitoid samples. Fields of within plate granite (WPG), ocean ridge granite (ORG), volcanic arc granite (VAG) and collision granite (COLG) are from Pearce et al (1984).

One of the most popular classifications of granitoid rocks is the I- and S-type granitoid classification. These two contrasting granite types were recognized by

(Chappell and White 1974) as they proposed a genetic subdivision of the granitic rocks into those extracted from sedimentary protoliths (S-type) and those derived from igneous source rocks (I-type). Granites were interpreted as being derived by partial melting with composition that directly reflects their source compositions. Another group of granites has been designated A-type by (Loiselle and Wones 1979). The term A-type granite was used to emphasize the anorogenic tectonic setting, the relatively alkaline composition, and the supposed anhydrous character of the magmas. Based on $Zr + Nb + Ce + Y$ vs $(Na_2O + K_2O)$ diagram (Whalen et al 1987), the studied granitoid rocks fall in three fields. The syn tectonic granite samples lie within the I- and S- type granite fields and some samples fall in the field of highly fractionated I-type granite (Fig. 3.9). On the other hand, all the post-tectonic granite samples plot in the A- type granite field (Fig. 2.9).

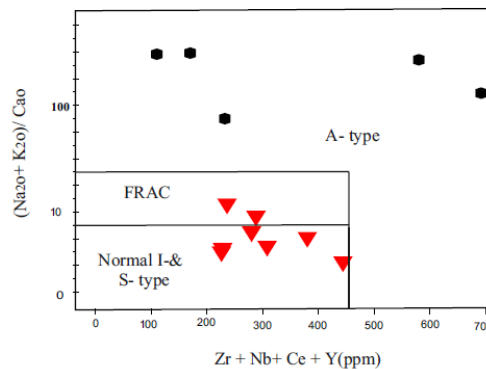


Fig 2.9: $Zr + Nb + Ce + Y$ vs $(Na_2O + K_2O)$ diagram after (Whalen et al 1987). The syn-tectonic granite samples lie within the field of I- & S- type granite and the post- tectonic granite samples plot in the field of A- type granite.

(Eby 1990, 1992) subdivided the A-type granites into two groups: A1, which represents differentiates of mantle-derived oceanic island basalts (anorogenic or rift zone), and A2, which represents crustal derived granite of a post-orogenic setting. On the Y/Nb vs. Rb/Nb diagram (Eby, 1990, 1992), which can be used to distinguish between the A1 (rift-related) and A2 (post-collision) sub-types of the A-type granites, most of studied granites plot in the A1 and A2 sub-type granites (Fig. 2.10). Moreover, the SiO_2 vs Al_2O_3 discrimination diagram of (Maniar and Picoli 1989), which is designed to separate the granitoid rocks into Island arc granite (IRG), continental arc granite (CAG), continental collision granite (CCG), rift related granite (RRG), post-orogenic granite (POG) and continental epirogenic uplift granite (CEUG). Most of the syn-tectonic granite samples fall in the CAG+ IRG+ CCG (volcanic arc field) whereas the post-tectonic granite samples plot in the field of post-orogenic granite (POG) (Fig. 3.11).

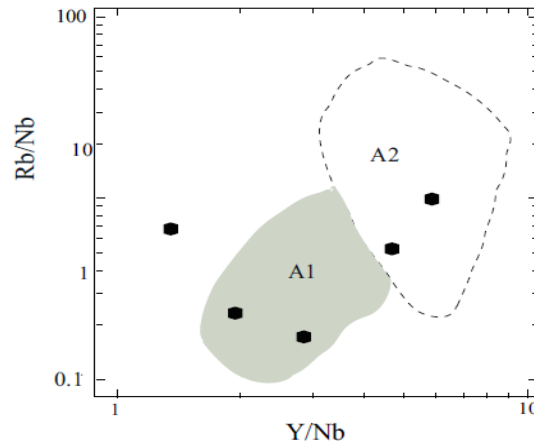


Fig. 2.10: Y/Nb vs. Rb/Nb diagram (Eby, 1992) distinguishing between the A1 (rift-related) and A2 (post-collision) subtypes of the A-type granites.

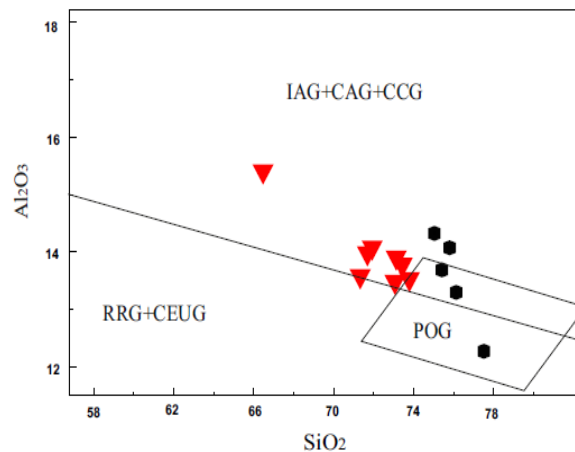


Fig. 2.11: SiO₂ vs. Al₂O₃ discrimination diagram of Maniar and Picoli (1989). The syn-tectonic granite samples fall in the volcanic arc field (CAG+ IRG+ CCG) whereas the post-tectonic granite plots in the post-orogenic granite (POG) field.

3.1 . Petrogenesis of the granitoid rocks

The field, petrographic and geochemical data (major, trace and rare earth elements) of the studied granitoid rocks indicates that they are syn-orogenic granitoids and post-orogenic granite. The syn-orogenic granitoids vary from granodioritic to granitic in composition. They are massive to slightly foliate with structural evidence, at the contact zone with the host rock, suggesting emplacement before the late folding phase (i.e. syn-tectonic). The post-orogenic granites intrude the metavolcano-sedimentary rocks and the syn-tectonic granite. They are of pink colour, coarse-grained, non-foliated, and contain quartz, plagioclase and K-feldspar, with little amount of mica and hornblende.

3.1.1. Syn-tectonic granitoids

The syn-tectonic granitoids are represented by granodiorite-granite suite, which shows chemical characteristics of calc-alkaline subduction-related magma and can be regarded as I-type products (Figs. 2.6 – 2.9). The primitive nature of the original magma that produced the syn-tectonic granodiorite-granite suite is evident from the very low Rb/Sr (0.09–0.35), Nb (3–7 ppm) as can be seen in Table 3.

Materials with such features are found only in the upper mantle as garnet lherzolite or in the lower crust. The latter may represent eclogite or amphibolite that has been formed earlier as part of older arc-back-arc crust. Thus the primary melt of the granodiorite may have formed either by fractionation of a more mafic mantle-derived magma or by partial melting of a depleted lower or middle crust. It cannot be a direct partial melt of the mantle peridotite (Wyllie, 1984). The geochemical data show marked continuities in major and trace element abundances versus SiO₂ (Figs. 2.2 and 2.3) suggesting that all varieties of the syn-tectonic granodiorite-granite suite are genetically related. The trend from the least evolved granodiorite sample (SiO₂=66 %) to the most evolved one (SiO₂=74%) is defined by decreasing Al₂O₃, CaO, MgO, Ba and Sr, and increasing alkalis, Rb, and Zr with increasing SiO₂ (Figs. 2.2 and 2.3). This evolution suggests fractionation through crystallization of plagioclase feldspar, amphibole, and magnetite. In the Arabian-Nubian Shield, calc-alkaline island-arc basalt magmas are represented by many metagabbro-diorite complexes, which thus documents the chemical evolution of basaltic magma and may represent a possible parent for the investigated granodiorite-granite suite through fractional crystallization.

In element variation diagrams (Figs. 2.2 and 2.3), there are inconsistent trends and compositional gaps between the post-collision granite and the syn-tectonic granite. Such geochemical variations indicate that both types of granite are genetically unrelated. For the post-collision granite, the ferroan character and the overall alkalic to alkali-calcic affinities of most rock types (Fig. 3.1a) are consistent with the original definition of A-type granitoids proposed by (Loiselle and Wones 1979) and as emphasized by Frost and (Frost 2001). The post-collision granites plot in the field of alkaline to alkali-calcic magmas (Fig 3.1b). This evidence suggests an important petrogenetic connection between the different A-type granitic rocks.

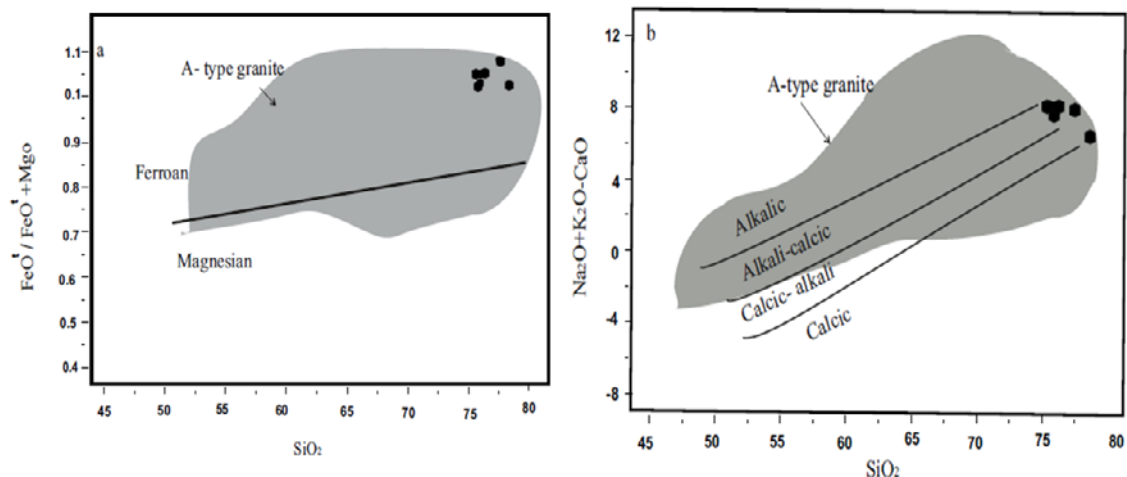


Fig. 3.1: Whole rock variation diagrams of the studied post-collision granite, (a) SiO₂ versus FeO/(FeO + MgO) after Frost et al. (2001) showing the granitic rocks are ferroan, (FeO = total iron expressed as FeO); (b) SiO₂ versus modified alkali lime index (MALI = Na₂O + K₂O - CaO) after Frost et al. (2001) shows the alkali-calcic to alkalic character of the studied post-orogenic granite; the field of A-type granite in (a) and (b) after Frost et al. (2001).

Many petrogenetic models have been invoked to explain the mechanism of formation of A-type granites. These include:

- (1) Anatexis of melt depleted, I-type, lower crustal protoliths (Collins et al., 1982; Clemens et al., 1986);
- (2) Fractional crystallization of mafic parental magma (Stern and Hedge, 1985; Nardi and Bonin, 1991; Turner et al., 1992).
- (3) Dehydration partial melting of undepleted tonalitic to granodioritic source (Anderson, 1983; Sylvester, 1989; Creaser et al., 1991; Skjerlie and Johnston, 1993);

The high contents of LILE (Table 5.3) such as K_2O (3.67 – 4.71 wt%), Rb (26 – 289ppm), Ba (24 - 139ppm) and Th (2.4 - 11) reflect the relatively undepleted juvenile source for the investigated A-type granites, and preclude their derivation by anatexis of melt-depleted lower crust. The trace-element patterns of the studied A-type granites show marked enrichments in LILE, LREE, and Sr and depletions in Nb, and Ta (Fig. 2.5). These features were likely inherited from a mantle source metasomatized by melts/fluids released from a subducting slab (e.g., Gertisser and Keller, 2003; Kogiso et al., 2009; Turner et al., 1992), or modified by subducted sediments and associated fluids/melts (e.g., Stolz et al., 1988). Thus, the source of the studied A-type granites could be a mantle that was metasomatized by melts/fluids released from a subducting slab. The occurrence of coeval mantle-derived mafic igneous rocks in the study area, such as the fresh gabbro, could point to a juvenile contribution in the formation of the studied A-type granites. However, this model does not appear to be viable due to the predominance of the granites in volume over gabbros and the relative scarcity of intermediate rocks, which eclipse a magma differentiation model (Frost and Frost, 2011).

Thus, the studied A-type granites were generated by partial melting of a young crustal source, with subsequent fractionation of feldspars and mafic minerals during magmatic evolution. The heat required for such a partial melting can be accounted for mantle-derived, volatile-rich, undepleted melts. The volatiles from the upper mantle were also important agents of heat transfer, and sufficient for metasomatism and anatexing the young crustal rocks. These melts are related to decompression melting due to erosional uplifting following lithospheric delamination during the post-collisional stage of the ANS evolution. Upwelling asthenosphere through the slab window provided enhanced heat flux and triggered the magmatism (Geng et al., 2009).

The low La/Nb (0.12–0.39), Sr (10 – 19ppm) and low Eu/Eu* (0.11 – 0.56) indicate that the studied A-type granites are highly differentiated (Bau, 1996). Pronounced negative Eu anomalies (Fig. 2.4) require extensive fractionation of feldspar. Plagioclase fractionation should produce negative Sr and Eu anomalies, whereas K-feldspar separation is responsible for the negative Ba anomaly (Wu et al., 2002). The presence of strongly negative Eu, Sr, and Ba anomalies in the studied granites (Figs. 2.4 and 2.5) thus indicate fractionation of both plagioclase and K-feldspar. This is further confirmed by the positive correlation between Ba versus Eu/Eu* (Fig. 3.2a) and negative correlation between K/Rb and Eu/Eu* vs. Rb (Fig. 3.2b, c). Moreover, Al_2O_3 negatively correlates with SiO_2 (Fig. 3.2d), consistent with the inference that feldspar removal may have been responsible. Fe- and Ti-bearing minerals such as biotite, ilmenite, and titanite might have been other fractionating phases as suggested by the presence of negative Ti anomalies on the spider-diagram (Fig. 2.5).

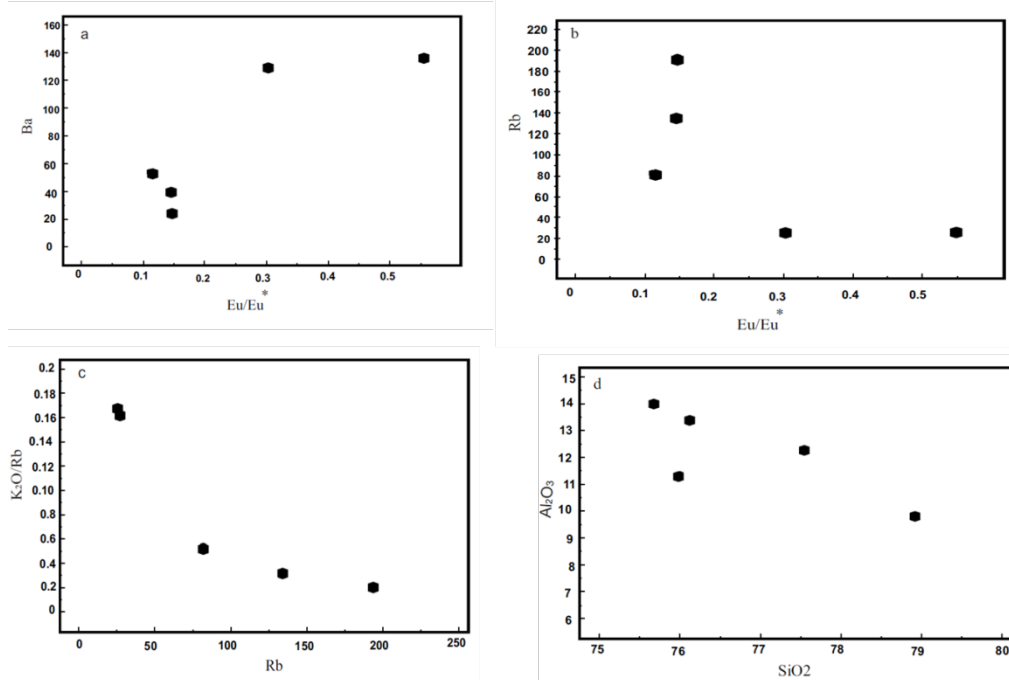


Fig. 3.2: (a) Eu/Eu* versus Ba diagram, (b) Eu/Eu* versus Rb diagram, (c) Rb versus K₂O/Rb diagram and (d) SiO₂ versus Al₂O₃ diagram, showing that fractionation of K-feldspar and plagioclase played an important role in the evolution of the studied A-type granites.

Table. 4: Calculations of the degree of the tetrad effect in the studied A-type granites according to [Irber \(1999\)](#).

Sample	A1	A3	B6-1	C18	B3
Ce	118.9	56.4	7.2	36.3	15.9
Ce(cn)	66.99	31.77	4.06	20.45	8.96
Nd	57.2	29.2	3.9	20.6	7.8
Nd(cn)	42.25	21.57	2.88	15.21	5.76
Pr	14.24	7.30	0.86	4.85	1.96
Pr(cn)	51.59	26.45	3.12	17.57	7.10
Tb	1.10	0.73	1.75	1.53	1.05
Tb(cn)	10.19	6.76	16.20	14.17	9.72
La	52.3	26.6	2.9	11.1	5.9
La(cn)	76.13	38.72	4.22	16.16	8.59
Gd	7.78	4.68	5.95	7.87	4.74
Gd(cn)	13.05	7.85	9.98	13.20	7.95
Ho	1.05	0.84	3.65	1.98	1.33
Ho(cn)	6.40	5.12	22.26	12.07	8.11
Dy	5.66	4.01	14.33	9.15	6.29
Dy(cn)	7.680	5.441	19.444	12.415	8.535
La(cn)2/3	17.962	11.445	2.612	6.391	4.194
Nd(cn)1/3	3.483	2.783	1.423	2.478	1.793
La(cn)1/3	4.238	3.383	1.616	2.528	2.048

Nd(cn)2/3	12.130	7.748	2.024	6.140	3.214
Gd(cn) 2/3	5.544	3.951	4.636	5.587	3.984
Ho(cn) 1/3	1.857	1.724	2.813	2.294	2.009
Gd(cn) 1/3	2.355	1.988	2.153	2.364	1.996
Ho(cn) 2/3	3.448	2.971	7.912	5.263	4.037
Ce/Cet	1.071	0.997	1.092	1.291	1.192
Pr/Prt	1.004	1.009	0.952	1.132	1.079
Tb/Tbt	0.989	0.993	1.242	1.105	1.215
Dy/Dyt	0.946	0.921	1.141	0.998	1.059
t1	1.037	1.003	1.020	1.209	1.134
t3	0.967	0.956	1.191	1.050	1.134
TE1,3	1.001	0.979	1.102	1.127	1.134

Although fractionation of feldspars and biotite may have caused some of the compositional variations in the studied granites, the tetrad effect on REE patterns (Fig. 2.4; Table 4) cannot be explained by such fractionation. The tetrad effect can cause a split of chondrite-normalized REE patterns into four segments (Irber, 1999) called tetrads (first tetrad, La–Ce–Pr–Nd; second tetrad, Pm–Sm–Eu–Gd; third tetrad, Gd–Tb–Dy–Ho; fourth tetrad, Er–Tm–Yb–Lu). The segments are either M-shaped (convex) or W-shaped (concave) lanthanide distribution patterns (Masuda et al. 1987). (Monecke et al. 2002) mentioned that the tetrad effect in granite lanthanide patterns can be attributed to fractional crystallization during granite differentiation or, to a characteristic of magma–fluid systems that develop during late stage granite crystallization (McLennan 1994; Kawabe 1995; Irber 1999). Irber (1999) showed that mineral fractionation alone is unlikely to cause the tetrad effect in granitic REE patterns because these could not be generated in Rayleigh fractionation calculations. Therefore, Irber (1999) argued that the tetrad effect of granite samples must have resulted from interaction of the granitic melt with a coexisting fluid at a late stage of crystallization after these split into magma and fluid subsystems. Moreover, (Jahn et al. 1993, 2001) emphasized that REE tetrad effects are not common and are most visible in late magmatic differentiates. This effect occurs typically in highly evolved magmatic systems, which are rich in H₂O and CO₂ and fluid-mobile elements such as Li, B, F and Cl (e.g., London 1986a, b, 1987, 1992, London et al. 1988).

For the studied granites, plotting ratios of K/Rb, Zr/Hf, and Sr/Eu versus the TE1,3 (tetrad effect; Fig. 3.3) help identify important controls on trace element behavior (Irber 1999). On the K/Rb versus TE1,3 diagram (Fig.3.3a), the studied granite samples display a negative correlation, and most samples have TE1,3≥1 and K/Rb from 150 to 1400. Such variation is considered to indicate mineral growth in the presence of aqueous fluids (Shearer et al. 1985; Clarke 1992). The Zr/Hf ratios range from 8 to 65 and negatively correlate with TE1, 3 (Fig. 3.3b), which is characteristic of petrogenetic systems involving F-bearing fluids (Bau 1996; Irber 1999). The strong decrease in Eu concentrations with tetrad effect is seen in Sr/Eu ratios (Fig.3.3c) and shows high value at TE1,3>1.10, which is opposite to the trend expected if mineral fractionation is dominant (Irber 1999). Thus, the strong Eu depletion in late stage of granite crystallization may indicate a preferential Eu fractionation into a coexisting aqueous fluid phase (Muecke and Clarke 1981). On the basis of these considerations, it is suggested that crystal fractionation and fluid–rock interaction are the main control of the trace element distribution in the studied post-orogenic A-type granites.

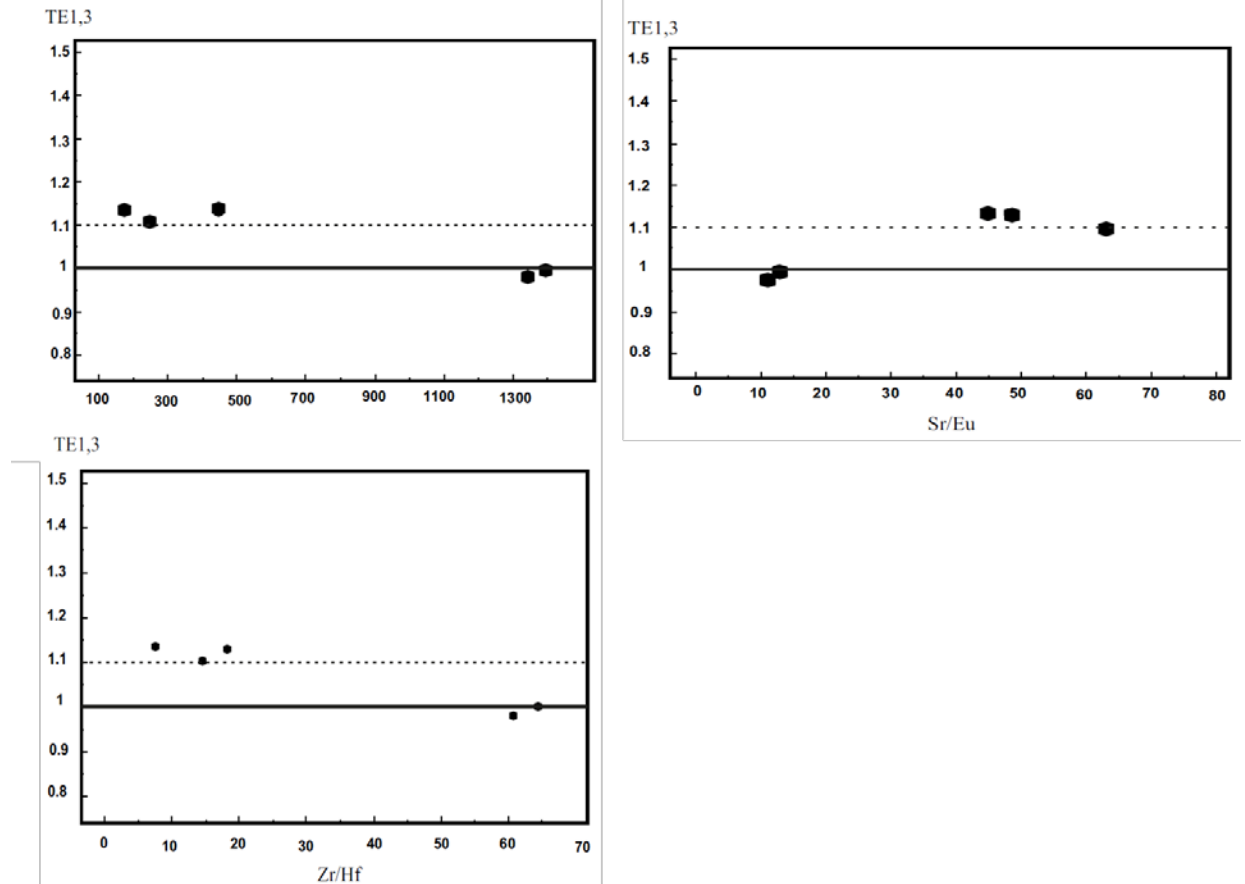


Fig. 3.3: Tetradeffect (TE1, 3) versus K/Rb, Zr/Hf, and Sr/Eu. The straight line mark the chondritic value, and the dashed lines define the boundary to clearly visible tetradeffects (TE1, 3[1.10) after (Irber 1999).

Conclusion:

The study area has been extensively intruded by syn- to late-tectonic plutons, which are intruded into the metavolcano-sedimentary sequence and vary in rock composition from granodioritic to granitic. The syn tectonic granite samples lie within the I- and S- type granite fields and some samples fall in the field of highly fractionated I- type granite. The trend from the least evolved granodiorite sample ($\text{SiO}_2=66\%$) to the most evolved one ($\text{SiO}_2=74\%$) is defined by decreasing Al_2O_3 , CaO, MgO, Ba and Sr, and increasing alkalis, Rb, and Zr with increasing SiO_2 . This evolution suggests fractionation through crystallization of plagioclase feldspar, amphibole, and magnetite. The primitive nature of the original magma that produced the studied granodiorite-granite suite is evident from the very low Rb/Sr (0.09–0.35), Nb (3–7 ppm), which reflect either garnet lherzolite mantle source or amphibolitic lower crust source. Thus the primary melt of the granodiorite may have formed either by fractionation of a more mafic mantle-derived magma or by partial melting of a depleted lower crust. On the other hand, all the post-tectonic granite samples plot in the A- type granite field. Most of the syn-tectonic granite samples fall in the CAG+ IRG+ CCG (volcanic arc field) whereas the post-tectonic granite samples plot in the field of post-orogenic granite. The ferroan character and the overall alkalic to alkali-calcic affinities of most rocks are consistent with the original definition of A-type granitoids proposed by Loiselle and Wones (1979) and as emphasized by Frost and

Frost (2011). It is suggested that the studied A-type granites were generated by partial melting of a young crustal source, with subsequent fractionation of feldspars and mafic minerals during magmatic evolution. These melts are related to decompression melting due to erosional uplifting following lithospheric delamination during the post-collisional stage of the ANS evolution. On the basis of geochemical variations, it is suggested that crystal fractionation and fluid–rock interaction are the main control of the trace element distribution in the studied post-orogenic A-type granites.

Reference:

Abu Fatima, M.(1992): *Magmatic and tectonic evolution of the granite - greenstone sequence of the Sinkat area, Red Sea Province. NE Sudan. Unpublished M.phil thesis, Department of Geology, University of Portsmouth, UK. 120-199.*

Anderson, J. L. (1983): Proterozoic anorogenic granite plutonism of North America. Geological Society of America, Memoirs, 133-154.

Barker F. and Arth J. G.(1976): *Generation of trondhjemitic – Tonalitic liquids and Archean bimodal trondhjemite- basalt suites.* Geology, 4:596-600.

Chappell B. W. and White A.J.R. (1974): *Two contrasting granite types.* Pacific Geology. 8: 172 – 174.

Clemens, J.D., Holloway, J.R., and White, A.J.R. (1986): Origin of an A-type granite: Experimental constraints: American Mineralogist, v. 71: 317-324.

Collins, W. J., Beams, D., White, J. R. & Chappell, B.W. (1982): Nature and origin of A-type granites with particular reference to south-eastern Australia. Contributions to Mineralogy and Petrology, 200:80-189.

Creaser, R.A., Price, R.C., Wormald, R.J.(1991): A-type granites revisited: assessment of residual-source model. Geology 19: 163–166.

Deer, W.A.; Howie, R.A. and Zussman, J., (1992). *An introduction to the rock forming minerals. 2nd edn.* Longman Scientific & Technical Group LTD, England. 696p.

Eby, G.N. (1990): *The A-type granitoids: a review of their occurrence and chemical characteristics and speculations on their petrogenesis.* Lithos 26:115–134.

Eby, GN. (1992): *Chemical subdivision of the A-type granitoids: petrogenetic and tectonic implications.* Geology 20: 641–644.

Frost, C.D., Frost, B.R., (2001): On ferroan (A-type) granitoids: their compositional variability and modes of origin Journal of Petrology. 52: 39–53

Hall, A. (1987): *Igneous Petrology, Longman.* Harlow, 573 pp.

Geng, H.Y., Sun, M., Yuan, C., Xiao, W.J., Xian, W.S., Zhao, G.C., Zhang, L.F., Wong, K., Wu F.Y.(2009): Geochemical, Sr, Nd and zircon U— Pb Hf isotopic studies of Late Carboniferous magmatism in the West Junggar, Xinjiang: implications for ridge subduction. Chemical Geology 266: 364–389.

Gertisser, R. & Keller J. (2003): Trace element and Sr, Nd, Pb and O isotope variations in medium-K and high-K volcanic rocks from Merapi Volcano, Central Java, Indonesia: evidence for the involvement of subducted sediments in Sunda Arc magma genesis. *Journal of Petrology*, 44 (3): 457-489.

Klemenic, P. M. Poole, S., Ali, S. E. M. (1985): *The geochemistry of late upper Proterozoic volcanic groups in the Red Sea Hills of NE Sudan – evolution of a late Proterozoic volcanic arc system.* *Journal of Geological Society of London*, 142: 1221-1233.

Kogiso, T., Hirschmann, M.M., Pertermann, M. (2004): High-pressure partial melting of mafic lithologies in the mantle. *Journal of Petrology* 45 (12), 2407–2422.

Loiselle, M.C. and Wones, D.R. (1979): *Characteristic and origin of anorogenic granites, Geological Society of America. Abstract.* With programs 11: 468 pp.

Maniar, P.D. and Piccoli, P.M. (1989): *Tectonic discrimination of granitoids.* Geological Society of America, Bull. 101: 635 – 643.

Moghazi A.M. (1994): *Geochemical and radiogenic isotope studies of some basement rocks at the Kid area southeast Sinai, Egypt.* PhD, geology department-faculty of science, Alexandria University, Egypt, 377pp.

Nardi, L.V.S and Bonin B. (1991): Post-orogenic and non-orogenic alkaline granite associations: the Saibro intrusive suite, southern Brazil - A case study. *Geological Chemistry* 92: 197-212.

Nour, S ,M. (1983): *Studied the geology of the dyke swarms of the khor Sagesota area. North Red Sea Hills Sudan.* M.Sc. Thesis, Unpubl, 213pp.

Pearce, J.A. (1982): *Trace element characteristic of lavas from destructive plate boundaries.* In Thorpe, S. (Editors.), *Andesites*, Chichester, Wiley: 525 – 548.

Pearce, J. A. Harris, N. B. W. and Tindle, A. G. (1984): *Trace element discrimination diagrams for the tectonic interpretation of granitic rocks.* *Journal of Petrology*, 25: 63 – 81.

Skjerlie, K. P. & Johnston, A. D. (1993): Fluid-absent melting behavior of an F-rich tonalitic gneiss at mid-crustal pressures: Implications for the generation of anorogenic granites. *Journal of Petrology* 34: 785-815.

Streckeisen, A. And Le Maitre, R. W. A. (1979): *Chemical approximation to the modal QAPF classification of the igneous rocks.* *Neues-Jahrbuch- Mineralogie – Abhandlungen*, 136 (1979): 169- 206.

Stern, R.J., Hedge, C.E. (1985): Geochronologic and isotopic constraints on Late Precambrian crustal evolution in the Eastern Desert of Egypt. *American Journal of Sciences* 285: 97–127.

Stolz, A.J., Vame, R., Wheller, G.E., Foden, J.D., Abbott, M.J. (1988): The geochemistry and petrogenesis of K-rich alkaline volcanics from the Batu Tara volcano, eastern Sunda Arc. *Contributions to Mineralogy and Petrology* 98: 374–389.

Sun, S. S. and McDonough, W. F. (1989): *Chemical and isotopic systematics of oceanic basalts; implications for mantle composition and processes.* In: *Magmatism in the ocean basins.* Saunders, A.D, and Norry, M.J. (Editors), Geological Society of London, 42: 313-345.

Sylvester, P.J. (1998): *Post-collisional strongly peraluminous granites.* Lithos 45: 29–44.

Turner, S.P., Foden, J.D., Morrison, R.S. (1992): Derivation of some A-type magmas by fractionation of basaltic magma: An example from the Padthaway Ridge, South Australia. Lithos 28: 151–179.

Vail, J.R. (1988): *Tectonics and evolution of the Proterozoic Basement of northeastern Africa.* In: *The Pan-African Belt of northeast Africa and adjacent areas.* El-Gaby, S. and Greiling, R.O. (Editors), F. Vieweg: Braunschweig, 195-226. {Eastern Sudan; tectonics, ophiolites; Proterozoic}.

Whalen, J.B., Currie, K.L., and Chappel, B.W. (1987): *A- type granites, geochemical characteristic, discrimination and petrogenesis.* *Contribution of Mineral & Petrology* .95: 407-419. Wilson, M. (1989): *Igneous Petrogenesis.* Unwin Hyman, London, 460 pp.

Wood, D.A. (1979): *A variably veined suboceanic upper mantle- genetic significance for mid – ocean ridge basalts from geochemical evidence.* *Geology* 7: 499 – 503.

Wyllie P. J. et al., Philosophical Transactions A, (1984): Constraints Imposed by Experimental Petrology on Possible and Impossible Magma Sources and Products. *Philosophical Transactions of the Royal Society of London, Series A.* 310: 439-456.

Younis, M.O.H, (2010): *Lithochemical Methods in prospecting and exploration for gold deposits in Derudeib area. Red Sea Hills. NE Sudan.* M.Sc. Thesis, School of Applied Earth Sciences. Faculty of Science and Technology. Al Neelain University, 80 pp.